

OPEN ACCESS

Experimental wind tunnel testing of linear individual pitch control for two-bladed wind turbines

To cite this article: Edwin van Solingen *et al* 2014 *J. Phys.: Conf. Ser.* **524** 012056

View the [article online](#) for updates and enhancements.

You may also like

- [Overview and Design of self-acting pitch control mechanism for vertical axis wind turbine using multi body simulation approach](#)

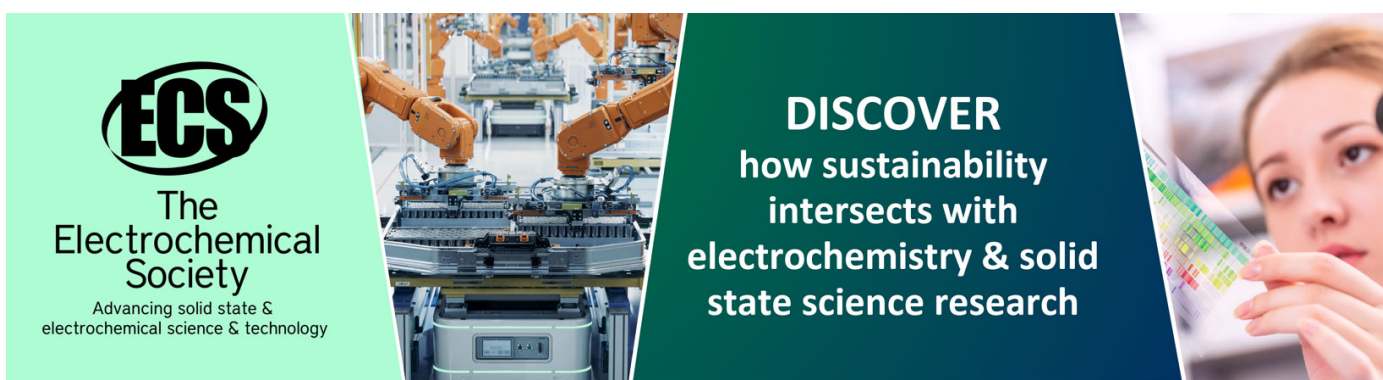
Prasad Chougule and Søren Nielsen

- [Design of a two-bladed 10 MW rotor with teetering hub](#)

M Civati, L Sartori and A Croce

- [Wind Turbine Load Mitigation based on Multivariable Robust Control and Blade Root Sensors](#)

A Díaz de Corcuera, A Pujana-Arrese, J M Ezquerro *et al.*



ECS
The
Electrochemical
Society
Advancing solid state &
electrochemical science & technology

DISCOVER
how sustainability
intersects with
electrochemistry & solid
state science research

Experimental wind tunnel testing of linear individual pitch control for two-bladed wind turbines

Edwin van Solingen, Sachin Navalkar and Jan-Willem van Wingerden

Delft Center for Systems and Control, Delft University of Technology, Delft, The Netherlands

E-mail: E.vanSolingen@tudelft.nl

Abstract. In this paper Linear Individual Pitch Control (LIPC) is applied to an experimental small-scale two-bladed wind turbine. LIPC is a recently introduced Individual Pitch Control (IPC) strategy specifically intended for two-bladed wind turbines. The LIPC approach is based on a linear coordinate transformation, with the special property that only two control loops are required to potentially reduce all periodic blade loads. In this study we apply LIPC to a control-oriented small-scale two-bladed wind turbine, equipped with, among others, two high-bandwidth servomotors to regulate the blade pitch angles and strain gauges to measure the blade moments. Experimental results are presented that indicate the effectiveness of LIPC.

1. Introduction

Capital and operational costs associated with offshore wind energy are targeted to be reduced by at least 20% by 2020 [1], and hence commercial wind turbines are designed to be larger and also increasingly more flexible. For rotating structures of the scale of modern wind turbines, it becomes necessary to implement some form of active blade load control methodology to withstand the increased dynamics loads occurring over the wind turbine lifetime. One such methodology to mitigate wind turbine loads is Individual Pitch Control (IPC).

In the past decade, IPC has received considerable attention in literature. Most notable are the contributions by Bossanyi in [2, 3] and more recently in [4]. Numerous extensions and modifications for IPC have been reported in [5–12]. Typically, all these papers concentrate on three-bladed wind turbines, however since the focus on onshore wind energy shifts to offshore wind energy, two-bladed wind turbines are becoming attractive, the main reasons being that the visual and noise impacts disappear. Also, two-bladed wind turbines save the material of one blade and have some installational advantages. Currently, several companies are developing two-bladed wind turbines [13].

A study of IPC for two-bladed wind turbines showed that by using a different coordinate transformation, only two controllers are required to be able to mitigate all periodic blade loads [14]. For reference, the conventional IPC approach using the Coleman transformation, requires two controllers for each blade load harmonic that one wants to alleviate. The IPC approach for two-bladed wind turbines proposed in [14] uses a linear coordinate transformation and it is referred to as Linear Individual Pitch Control (LIPC). Similar to the Coleman transformation, also the linear coordinate transformation decouples the transformed signals, allowing for Single-Input Single-Output control design. A simulation study indicated that both IPC methods achieve similar load reduction levels [14].





Figure 1. Small-scale two-bladed wind turbine

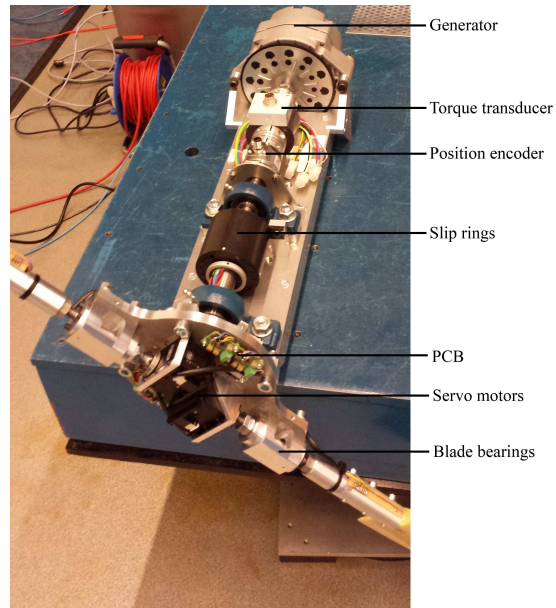


Figure 2. Close-up of the drivetrain and hub

To be able to test (advanced) control design techniques, a small-scale two-bladed wind turbine was designed and constructed. The small-scale turbine has a variety of sensors and actuators, most notably two high-bandwidth servomotors for individual blade pitching. Testing control algorithms on such an experimental wind turbine can be regarded as an intermediate step between theory and real-world application. In the past, wind tunnel tests were carried out in the context of a downwind free yawing wind turbine [15]. Furthermore, model-predictive control has been used to alleviate gust loads by measuring the wind speed upwind of the wind turbine [16] and load reduction capabilities by means of blades equipped with actuator flaps (smart rotor) were assessed in [17]. The design of a scaled-down aero-servo-elastic wind tunnel model of the 3 MW Vestas V90 wind turbine is described in [18]. The small-scale wind turbine presented in this paper is an evolution of the experimental setup used in [16, 19].

The main contributions of this paper are:

- Describing the experimental small-scale two-bladed wind turbine;
- Demonstrating the LIPC strategy on the small-scale two-bladed wind turbine.

The description of the small-scale wind turbine is given in Section 2. The LIPC strategy is outlined in Section 3 and the results of the LIPC applied to the experimental wind turbine are given in Section 4. The last section gives the conclusion.

2. Experimental setup

Before validating control algorithms on real-world applications, an intermediate step to real-world application is to test control algorithms using an experimental setup. For that reason, a small-scale two-bladed wind turbine has been built. The main purpose of the small-scale wind turbine is to be able to test novel and advanced control algorithms on a practical setup, which contains all the control degrees of freedom of a wind turbine. The small-scale wind turbine has a rotor diameter of approximately 1.6 m and the generator has a maximum electrical energy output of roughly 300 W. The typical rotational speed is between 200 rpm and 600 rpm.

In Figure 1, a photograph of the small-scale two-bladed wind turbine in the Open Jet Facility of the Delft University of Technology is shown. A close-up of the drivetrain and rotor hub is

Table 1. Important frequencies of the experimental setup

Description	Frequency [Hz]	Rotational speed [rpm]
1P frequency at $v = 6.5$ m/s	3.9	230
1P frequency at $v = 7.5$ m/s	4.6	275
1P frequency at $v = 9.5$ m/s	6.6	395
Blade structural frequency	15	—
Tower structural frequency	5.5	—

shown in Figure 2. The following components are visible from top to bottom in Figure 2: generator, torque transducer, position encoder, slip rings and two servomotors connected to the blade roots. In the rotor hub also two PCB's, with an electrical bridge configuration for the strain gauges, are mounted. The blade roots are connected to the shaft through two bearings, i.e., a radial and axial bearing. The blades that have been used were also used in previous experiments [15, 19].

2.1. Main features of the experimental setup

The experimental setup exhibits a variety of features which are described below.

Individual blade pitch Two high-bandwidth servomotors mounted in the rotor allow for blade pitch control. With the help of system identification tools it was observed that the servomotors reach a bandwidth over 15 Hz, both in no-load conditions as well as under load.

Strain gauges in each blade Each blade is equipped with two strain gauges located close to the root and approximately halfway the blade, respectively. The strain voltages serve as a measure for the blade moments.

Torque control The electrical energy generated by the generator is dissipated in a dump load with variable resistance. In other words, by changing the resistance of the dump load, the current and, hence, the generator torque can be controlled.

Position sensor The rotor azimuth is measured with a position encoder, which can also be used to obtain the rotor speed;

Torque sensor A torque transducer is installed such that the mechanical input can be measured and such that drivetrain loads can be measured;

Free yaw The wind turbine tower is mounted using two bearings (the upper bearing can be partly seen in Figure 1) and a clamp is used to fix the tower in a certain yaw direction. By releasing the clamp, free yaw is also possible [15].

Electrical output The electrical energy generated by the setup is monitored by a voltage and current sensor.

Design flexibility The wind turbine setup is designed such that it can be easily modified. For example, it is relatively easy to assemble different blades, possibly having multiple (additional) sensors and actuators (e.g., smart rotor flaps [17]).

In this study, the wind turbine is configured upwind and the yaw position is such that the rotor plane is perpendicular to the wind direction.

2.2. Frequencies of the experimental setup

The rotor speed in the experiments is not regulated by a torque or collective pitch controller. Instead, the dump load is set to a fixed resistance and the blades are set to a fixed blade pitch angle. Hence, for wind speed variations also the rotor speed will vary accordingly. This means

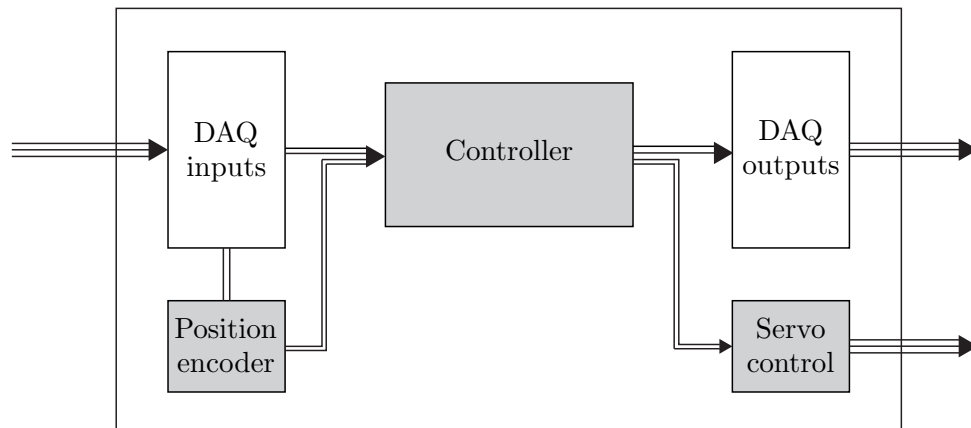


Figure 3. Interconnections of the DAQ and control system. The white blocks run at 2 kHz and the grey blocks run at 200 Hz. Rate transitions are used to ensure proper data propagation.

that for different wind speeds, the once-per-revolution frequency, i.e., the 1P frequency (and the harmonics thereof) will be different. The 1P frequency of the setup is listed in Table 1 for different wind speeds. Moreover, also the fundamental blade and tower structural frequencies are given.

2.3. Data acquisition and controller implementation

The above mentioned sensors and actuators of the setup are connected to a PC with data acquisition system (DAQ). All signals are acquired at 2 kHz and then passed through a first-order low-pass filter with cutoff frequency at 200 Hz to remove unwanted high frequency content. The rotor azimuth is obtained with an internal counter of the DAQ running at 200 Hz. The rotor azimuth signal is then converted to rotor speed by using a discrete derivative and is finally low-pass filtered with cutoff frequency at 10 Hz. The control algorithms run at a sample frequency of 200 Hz, so that computational effort is not an issue. The servo motors used to set the individual blade pitch also run at 200 Hz and make use of a dedicated serial communication card installed in the PC. Rate transitions ensure proper data propagation between the different blocks. A simplified overview of the DAQ with the control algorithms is shown in Figure 3. Notice that the rate transition blocks are not shown in the simplified diagram. The diagram shown in Figure 3 is implemented in MATLAB Simulink [20] and connected in real-time to the PC using xPC Target [21].

3. Individual Pitch Control

In the conventional approach of IPC for (two-bladed and three-bladed) wind turbines, the well-known Coleman coordinate transformation [22] is used. This technique has been validated in [4], both for two-bladed and three-bladed wind turbines. The Coleman transformation is non-linear and depends on the rotor azimuth. It transforms the rotating signals to a fixed non-rotating frame of reference, such that Linear Time-Invariant (LTI) controllers can be designed and implemented. It can be shown that the Coleman transformation for two-bladed rotors is singular [14]. Despite the singular transformation, field tests have indicated good performance [4, 23, 24]. Recently, in [14], a *linear* coordinate transformation specifically for two-bladed wind turbines was introduced. The main advantage of the linear coordinate transformation compared to the Coleman coordinate transformation is that it only requires two control loops to potentially reduce all (periodic) blade loads. For the Coleman transformation two controllers are required for each periodic blade load harmonic (i.e., 1P, 2P, etc.). As shown

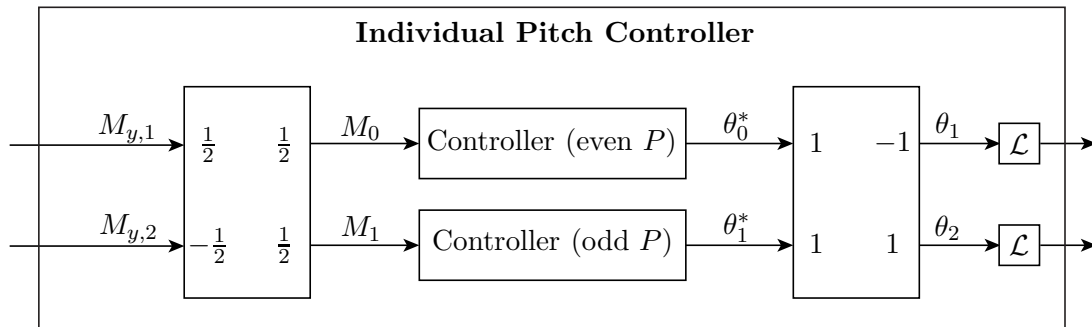


Figure 4. Linear Individual Pitch Control structure

in [14], a special property of the linear coordinate transformation is that it decouples the system such that SISO control design is possible.

The aim of the experiments is to mitigate the 1P and 2P blade loads. To this end, the details of the control approach and controller structure are outlined in the next subsection.

3.1. Linear coordinate transformation

In Figure 4, the structure of LIPC is outlined. The measured blade root moments $M_{y,1}$ and $M_{y,2}$ are passed through the forward linear coordinate transformation. Then the transformed signals M_0 and M_1 are input to two LTI controllers after which the pitch signals θ_0^* and θ_1^* are passed through the reverse linear coordinate transformation to obtain the pitch signals θ_1 and θ_2 . The linear coordinate transformation is given by

$$\begin{bmatrix} M_0 \\ M_1 \end{bmatrix} = \begin{bmatrix} 1/2 & 1/2 \\ -1/2 & 1/2 \end{bmatrix} \begin{bmatrix} M_{y,1} \\ M_{y,2} \end{bmatrix}, \quad (1)$$

where M_0 is the collective (coning) mode and M_1 is the reactionless differential (teetering) mode [25]. The reverse coordinate transformation is given by

$$\begin{bmatrix} \theta_1 \\ \theta_2 \end{bmatrix} = \begin{bmatrix} 1 & -1 \\ 1 & 1 \end{bmatrix} \begin{bmatrix} \theta_0^* \\ \theta_1^* \end{bmatrix}. \quad (2)$$

Note that the linear coordinate transformations are independent of rotor azimuth angle. The collective mode M_0 and the differential mode M_1 contain the summed and subtracted blade loads respectively. That is, the collective mode M_0 contains 0P and all even periodic blade load harmonics (2P, 4P, etc.) whereas the differential mode M_1 contains all odd periodic blade load harmonics (1P, 3P, etc.). The latter is shown in Figure 5 and Figure 6 after performing an open-loop experiment at a wind speed of $v = 6.5$ m/s. The rotational speed at this wind speed is approximately 230rpm. At this wind speed the 1P rotational frequency is 3.8 Hz (see Table 1). It can be observed in Figure 5 that the collective mode M_0 is dominated by the even harmonics. Furthermore, the differential mode M_1 is dominated by the odd harmonics. Notice that both the modes M_0 and M_1 contain harmonics which should ideally not be the corresponding mode. This can be attributed to differences in the strain gauge sensor calibration and asymmetry of the rotor and will not be further investigated in this work.

3.2. Linear Individual Pitch Control

In order to design the LIPC, the underlying dynamics from the blade pitch angle to the blade root moments need to be modeled. Since in our experiments the rotor speed is not regulated (i.e., there is no collective pitch control or torque control), the periodic loads vary with wind speed.

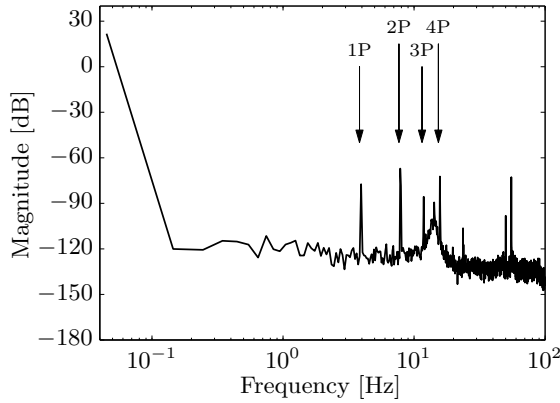


Figure 5. Power spectrum of M_0

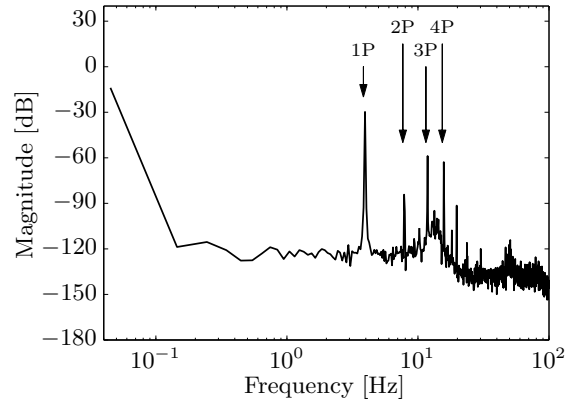


Figure 6. Power spectrum of M_1

To this end, we need to obtain a model for each wind speed considered. To do so, we have applied system identification techniques [26].

The aim in our experiments is to reduce the 1P blade loads and the 2P blade loads. Hence, a controller in the collective mode should target the 2P load and a controller in the differential mode M_1 should target the 1P load. To do so, the following fixed controller structure (also see [27]) for the collective mode M_0 is used

$$C_{M_0}(s) = K_{M_0} \times \mathcal{H}_{M_0}(s) \times \text{NF}_{\text{inv},2\text{P}}(s) \times \mathcal{L}_{M_0}(s), \quad (3)$$

where K_{M_0} is a static gain, $\mathcal{H}_{M_0}(s)$ is a high-pass filter, $\text{NF}_{\text{inv},2\text{P}}(s)$ an inverted notch filter at the 2P frequency, and $\mathcal{L}_{M_0}(s)$ a low-pass filter. A similar structure is used for the differential mode M_1

$$C_{M_1}(s) = K_{M_1} \times \mathcal{H}_{M_1}(s) \times \text{NF}_{\text{inv},1\text{P}}(s) \times \mathcal{L}_{M_1}(s). \quad (4)$$

The inverted notch filter passes only the desired rotational frequency such that control action at the desired frequency ω is obtained. The low-pass and high-pass filters are chosen such that any unwanted frequency content below or above the desired rotational frequency ω is filtered out of the control signal. The controller structure is schematically depicted in Figure 7.

The parameterization of the high-pass filters, inverted notch filter and low-pass filter is as follows

$$\mathcal{H}(s, K_{\mathcal{H}}, \tau_{\mathcal{H}}) = K_{\mathcal{H}} \frac{s}{\tau_{\mathcal{H}}s + 1}, \quad (5)$$

$$\text{NF}(s, \zeta, \beta_{\text{inv}}) = \frac{s^2 + 2\omega\zeta s + \omega^2}{s^2 + 2\omega\beta s + \omega^2}, \quad (6)$$

$$\mathcal{L}(s, K_{\mathcal{L}}, \tau_{\mathcal{L}}) = K_{\mathcal{L}} \frac{1}{\tau_{\mathcal{L}}s + 1}, \quad (7)$$

where $K_{\mathcal{H}}, K_{\mathcal{L}}$ are static gains, $\tau_{\mathcal{H}}, \tau_{\mathcal{L}}$ are time constants and ζ, β damping parameters. For the $v = 9.5 \text{ m/s}$ wind case the controller parameters values are respectively $7.09 \times 10^{-2}, 3.50 \times 10^{-1}, 1.59, 3.41 \times 10^{-4}, 2.91 \times 10^{-3}, 6.63 \times 10^3$ for the M_0 controller (2P) and $2.90 \times 10^0, 1.05 \times 10^{-3}, 1.59, 2.95 \times 10^{-2}, 3.52 \times 10^{-3}, 6.82 \times 10^3$ for the M_1 controller (1P).

4. Results

The experiments were carried out in the Open Jet Facility at the Delft University of Technology. The wind tunnel is a closed circuit capable of generating wind speeds up to 33 m/s at very low

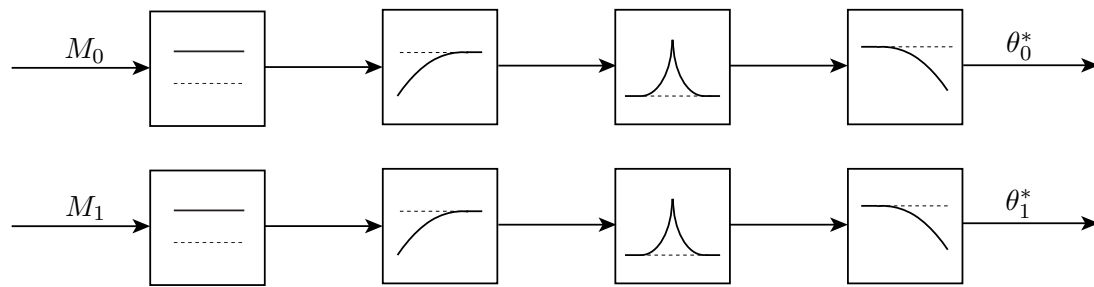


Figure 7. Schematic overview of the structure of Linear Individual Pitch Control (LIPC). The control blocks from left to right: static gain, high-pass filter, inverted notch filter, low-pass filter

turbulence levels. During the experiments, the small-scale wind turbine was used with the following conditions. As mentioned in Section 2, the wind turbine is configured upwind and the rotor plane is perpendicular to the wind direction (i.e., no yaw misalignment). The electrical dump load was set such that it has maximum resistance (which means a low current and, hence, low torque) and the collective blade pitch angle was set to a fixed angle. Therefore, as the rotor speed is not regulated, the rotational speed varied with wind speed. Three different wind speeds v are considered: 6.5 m/s, 7.5 m/s, and 9.5 m/s for which the rotor speed is roughly 230 rpm, 275 rpm, and 395 rpm, respectively. The signals considered for control are the measured strain gauge voltages of each blade and the blade pitch angle setpoint of each servomotor. Hence, the blade moments $M_{y,1}$ and $M_{y,2}$ are taken as the measured strain gauge voltages, which we denote by $V_{y,1}$ and $V_{y,2}$, respectively. The strain gauge signals are low-pass filtered at 200 Hz to remove any unwanted high frequency content and the controller ran at a sampling frequency of 200 Hz (refer to Section 2 for details of the DAQ and control system).

In this study, the following cases are considered

- (i) LIPC with 1P blade load control. This means that only the controller (see Eq. (4)) in the differential mode M_1 was used. This controller is denoted by LIPC-1P.
- (ii) LIPC with 1P and 2P blade load control. In this case both the controller (see Eq. (4)) in the differential mode M_1 and the controller (see Eq. (3)) in the collective mode were used. This controller is denoted by LIPC-1P-2P.
- (iii) For comparison, we also introduce the case where no controller is active and denote this as the baseline case.

The results for the case of $v = 9.5$ m/s are depicted in Figure 8 - Figure 11. The figures were generated by resampling all signals from 2 kHz to 200 Hz and the power spectral density plots are frequency averaged. Table 2 lists the results based on the resampled signals for the three wind speeds.

In Figure 8 - Figure 9 the strain gauge voltages are shown for 1P blade load control. It can be observed that for blade 1 the 1P load is completely removed and for blade 2 the 1P load is almost removed. It can be observed that the 2P load in blade 2 is slightly increased by the 1P control action. Moreover, as a positive side effect of the 1P load reduction, also the 3P load almost completely disappears.

For the case of 1P and 2P blade load control (see Figure 10 - Figure 11), it can be seen that the reductions in both blades are rather similar when considering the 1P frequency. For the 2P frequency, the reduction is larger in blade 1. Since the 2P frequency is rather close to the structural eigenfrequency of the blades, the 2P control action comes at the cost of slightly exciting the structural mode. Comparing Figure 8 and Figure 10, the reduction at 2P comes at the cost of less reduction at 1P.

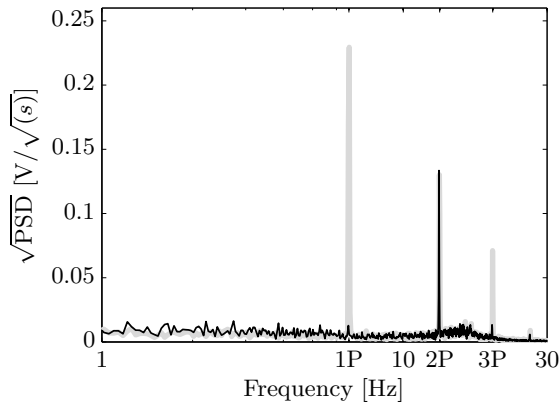


Figure 8. Blade 1 root strain $V_{y,1}$ for 1P load reduction at 9.5 m/s (grey: baseline, black: LIPC-1P)

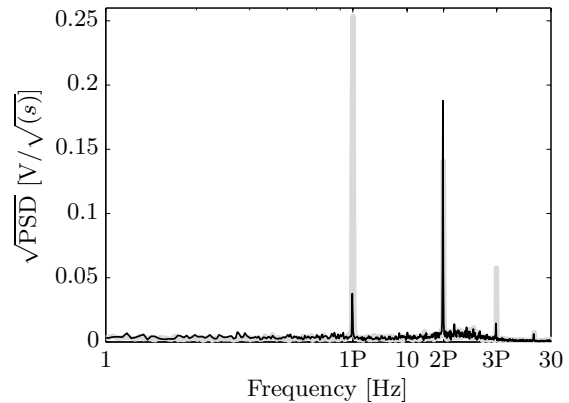


Figure 9. Blade 2 root strain $V_{y,2}$ for 1P load reduction at 9.5 m/s (grey: baseline, black: LIPC-1P)

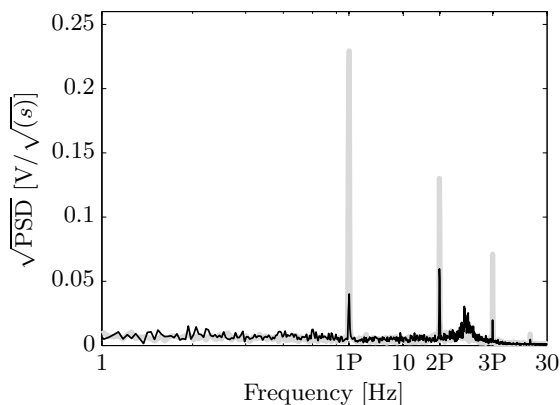


Figure 10. Blade 1 root strain $V_{y,1}$ for 1P and 2P load reduction at 9.5 m/s (grey: baseline, black: LIPC-1P-2P)

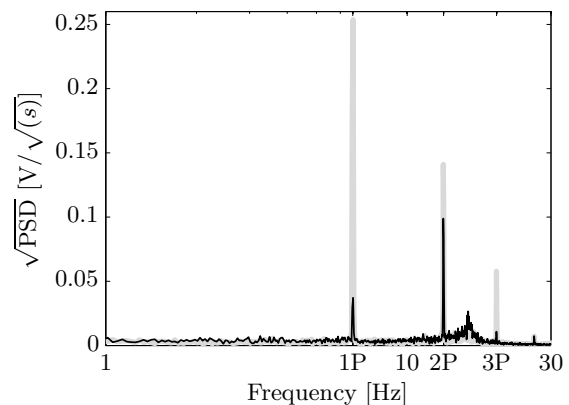


Figure 11. Blade 2 root strain $V_{y,2}$ for 1P and 2P load reduction at 9.5 m/s (grey: baseline, black: LIPC-1P-2P)

The standard deviation results in Table 2 show that the highest reductions were obtained at $v = 6.5$ m/s and that the added 2P control action in some cases gives a clear additional reduction with only slightly increased pitch effort. Furthermore, the tabulated results reveal that the reductions in blade 1 are higher than in blade 2, which can be attributed to a difference in control authority. That is, the lift profiles of both blades are different due to differences in the blade geometry. One case that requires some attention is the experiment with 1P and 2P control at 7.5 m/s. In this case adding 2P control action yields a significant reduction of the load reduction performance in blade 2 compared to the 1P control case. It was observed from the power spectral density plots that the 3P mode is excited by the 2P control action of blade 2, which causes a higher standard deviation. It should further be noted that the 3P frequency coincides with the structural blade mode, which further complicates the experiment.

Finally, the standard deviation of the rotor speed given in Table 2 indicates only small variations. For larger variations, the load reduction is likely to decrease, since the controllers were specifically tuned for the given wind speed and only apply control action at the rotor speed frequency. Therefore, when considering wind turbine application, the given LIPC approach is readily available for above-rated wind speeds [14]. However, for below-rated wind speeds, it is

Table 2. Experimental results for three wind speeds

v [m/s]	6.5	7.5	9.5
Standard deviation and percent reductions of blade 1 strain voltage $V_{y,1}$			
Baseline [V]	0.14	0.15	0.17
LIPC-1P [%]	56.9	45.1	42.6
LIPC-1P-2P [%]	67.1	52.3	44.4
Standard deviation and percent reductions of blade 2 strain voltage $V_{y,2}$			
Baseline [V]	0.14	0.16	0.18
LIPC-1P [%]	52.9	40.1	39.0
LIPC-1P-2P [%]	68.9	21.6	48.3
Standard deviation of blade 1 pitch angle θ_1			
LIPC-1P [deg]	0.59	0.50	0.39
LIPC-1P-2P [deg]	0.69	0.51	0.39
Standard deviation of blade 2 pitch angle θ_2			
LIPC-1P [deg]	0.58	0.49	0.38
LIPC-1P-2P [deg]	0.69	0.50	0.37
Standard deviation of the rotor speed			
Baseline [rpm]	0.87	1.05	1.54
LIPC-1P [rpm]	0.87	1.07	1.59
LIPC-1P-2P [rpm]	0.88	1.07	1.61

required to schedule the LIPC controllers on the rotor speed. This will not be further discussed in this paper.

It can be seen from the presented results, that there exist differences in the load reductions. The differences can be due to a variety of reasons:

- Although the blade geometry should be identical, it could visually clearly be seen that there were differences in the twist profile;
- Due to the blade differences, the same pitch actions for both blades are likely to result in different lift and thrust;
- The phase loss of the servomotors increases for higher frequencies;
- The sensor calibration and sensor position in the blade may not be perfect.

5. Conclusions

The experiments have indicated that the small-scale two-bladed wind turbine provides a convenient intermediate step for evaluating control algorithms in a real-world application. There were no failures during the experiments, which makes us believe it is a reliable test setup. The servomotors are shown to have a bandwidth high enough to deal with 1P and 2P periodic loads at rotor speeds over 400 rpm. The experimental setup features a wide range of sensors and has all the control degrees of freedom a wind turbine has. Moreover, the design is modular, so that, for example, including additional sensors and actuators for blade flap control is possible.

The main purpose of the experiments was to demonstrate a novel IPC strategy on a practical setup. It is shown that LIPC provides significant reductions at the 1P and 2P periodic blade loads with a simple controller structure. The results presented in this work can therefore be regarded as a first step in the proof of concept of the LIPC strategy.

Acknowledgements

The authors would like to thank Kees Slinkman, Simon Toet and Will van Geest for designing, manufacturing and assembling the experimental setup.

References

- [1] 2009 Far and large offshore wind summary (Accessed 2014) URL <http://flow-offshore.nl>
- [2] Bossanyi E A 2003 *Wind Energy* **6** 119–128
- [3] Bossanyi E A 2005 *Wind Energy* **8** 481–485
- [4] Bossanyi E A, Fleming P and Wright A D 2013 *Control Systems Technology, IEEE Transactions on* **21** 1067–1078
- [5] Geyler M and Caselitz P 2008 *Journal of Solar Energy Engineering* **130** 1–12
- [6] van Engelen T G 2009 Design model and load reduction assessment for multi-rotational mode individual pitch control (higher harmonics control) *European Wind Energy Conference*
- [7] Kanev S K and van Engelen T G 2009 Exploring the Limits in Individual Pitch Control *European Wind Energy Conference*
- [8] Selvam K, Kanev S, van Wingerden J W, van Engelen T and Verhaegen M 2009 *International Journal of Robust and Nonlinear Control* **19** 72–91
- [9] Wright A D, Fingersh L J and Stol K A 2009 Testing controls to mitigate fatigue loads in the controls advanced research turbine *Control and Automation, 2009. MED '09. 17th Mediterranean Conference on* pp 1275–1282
- [10] Wright A D and Stol K A 2010 Testing Further Controls to Mitigate Loads in the Controls Advanced Research Turbine *AIAA Aerospace Sciences Meeting*
- [11] Wright A D, Fleming P and van Wingerden J W 2011 Refinements and Tests of an Advanced Controller to Mitigate Fatigue Loads in the Controls Advanced Research Turbine *49th AIAA Aerospace Sciences Meeting*
- [12] Houtzager I, van Wingerden J W and Verhaegen M 2013 *Wind Energy* **16** 235–256 ISSN 1099-1824
- [13] 2-B Energy (Accessed April 2014) URL <http://2benergy.com/>
- [14] van Solingen E and van Wingerden J W 2014 *Wind Energy (Preprint we.1720)*
- [15] Verelst D R, Larsen T and van Wingerden J W 2012 Wind tunnel tests of a free yawing downwind wind turbine *Science of Making Torque from Wind*
- [16] Verwaal N W, van der Veen G J and van Wingerden J W 2014 *Wind Energy (Preprint we.1702)* ISSN 1099-1824
- [17] van Wingerden J W, Hulskamp A, Barlas T, Houtzager I, Bersee H, van Kuik G and Verhaegen M 2011 *Control Systems Technology, IEEE Transactions on* **19** 284–296 ISSN 1063-6536
- [18] Bottasso C L, Campagnolo F and Croce A 2011 Development of a wind tunnel model for supporting research on aero-servo-elasticity and control of wind turbines *13th International Conference on Wind Engineering*
- [19] Verelst D R, Larsen T J, Helge A M and Van Wingerden J W 2013 *Numerical and Experimental Results of a Passive Free Yawing Downwind Wind Turbine* Ph.D. thesis Delft University of Technology
- [20] Mathworks Simulink (Accessed 2013) URL <http://www.mathworks.com>
- [21] The MathWorks, Inc 2013 xPC Target User's Guide
- [22] Stol K A, Moll H G, Bir G S and Namik H 2009 A Comparison of Multi-Blade Coordinate Transformation and Direct Periodic Techniques for Wind Turbine Control Design *AIAA Aerospace Sciences Meeting*
- [23] Bossanyi E A and Wright A D 2009 Field testing of individual pitch control on the NREL CART-2 wind turbine *European Wind Energy Conference*
- [24] Bossanyi E A, Wright A D and Fleming P 2010 Controller Field Tests on the NREL CART2 Turbine Technical Report NREL/TP-5000-49085 National Renewable Energy Laboratory
- [25] Johnson W 1994 *Helicopter theory* Dover Books on Aeronautical Engineering Series (Dover Publications)
- [26] van der Veen G, van Wingerden J W, Bergamasco M, Lovera M and Verhaegen M 2013 *Control Theory Applications, IET* **7** 1339–1358
- [27] van Solingen E and van Wingerden J W 2014 Fixed-structure H_∞ control design for linear individual pitch control of two-bladed wind turbines *American Control Conference (ACC), 2014*